MNRAS **467,** 1526–1530 (2017)
Advance Access publication 2017 February 3

doi:10.1093/mnras/stx181

Confirmation of six Be X-ray binaries in the Small Magellanic Cloud

V. A. McBride,[1,2★] A. González-Galán,[3] A. J. Bird,[4] M. J. Coe,[4] E. S. Bartlett,[1,5] R. Dorda,[3] F. Haberl,[6] A. Marco,[3] I. Negueruela,[3] M. P. E. Schurch,[1] R. Sturm,[6] D. A. H. Buckley[2] and A. Udalski[7]

[1]*Department of Astronomy, University of Cape Town, Private Bag X3, Rondebosch 7701, South Africa*
[2]*South African Astronomical Observatory, PO Box 9, Observatory 7935, South Africa*
[3]*Departamento de Física, Ingeniería de Sistemas y Teoría de la Señal, Universidad de Alicante, Apdo. 99, E-03080 Alicante, Spain*
[4]*School of Physics and Astronomy, University of Southampton, Highfield, Southampton SO17 1BJ, UK*
[5]*ESO – European Southern Observatory, Alonso de Córdova 3107, Vitacura, Casilla 19001, Santiago de Chile, Chile*
[6]*Max-Planck-Institut für extraterrestrische Physik, Giessenbachstraße, D-85748 Garching, Germany*
[7]*Warsaw University Observatory, Aleje Ujazdowskie 4, PL-00-478 Warsaw, Poland*

Accepted 2017 January 19. Received 2017 January 18; in original form 2016 July 22

ABSTRACT

The X-ray binary population of the Small Magellanic Cloud (SMC) contains a large number of massive X-ray binaries, and the recent survey of the SMC by *XMM–Newton* has resulted in almost 50 more tentative high-mass X-ray binary (HMXB) candidates. Using probability parameters from Haberl and Sturm together with the optical spectra and timing in this work, we confirm six new massive X-ray binaries in the SMC. We also report two very probable binary periods of 36.4 d in XMM 1859 and of 72.2 d in XMM 2300. These Be X-ray binaries are likely part of the general SMC population, which rarely undergoes an X-ray outburst.

Key words: stars: emission-line, Be – Magellanic Clouds – X-rays: binaries.

1 INTRODUCTION

The Small Magellanic Cloud (SMC) has a unique population of X-ray binaries. It is entirely dominated by massive X-ray binaries, all of which have neutron star companions. This is a factor of ∼50 more X-ray binaries than would be expected, based on scaling by mass the Milky Way X-ray binary population. This excess is thought to be due to the higher star formation rate in the SMC, but possibly also influenced by the lower metallicity compared to the Milky Way (Dray 2006). The massive X-ray binary populations in the Milky Way, Large Magellanic Cloud (LMC) and SMC all have donor stars with spectral types predominantly earlier than B3 (Negueruela 1998; Negueruela & Coe 2002; McBride et al. 2008; Antoniou et al. 2009; Antoniou & Zezas 2016). Our current understanding of this limited mass range is through angular momentum loss during the evolution of the binary (Portegies Zwart 1995).

With a view to characterizing the X-ray population of the SMC, Haberl et al. (2012) have undertaken an X-ray survey of the SMC down to a limiting luminosity of 5×10^{33} erg s^{-1} (assuming a distance of 60 kpc to the SMC; Hilditch, Howarth & Harries 2005), with a wide coverage across the SMC (see fig. 3 in Haberl et al. 2012). Through the primary analysis of the point source X-ray data from this survey, Sturm et al. (2013) have generated a list of candidate high-mass X-ray binaries (HMXBs), which is presented in table 5 of their paper. Objects are classified as candidate HMXBs on the basis of their X-ray and optical colours. In particular, hard X-ray sources are classified as HMXBs when they have an optical counterpart in the magnitude range of $13.5 < V < 17$ with optical colours characteristic of an early-type star, and are not already identified with a known background active galactic nucleus. Forty-five X-ray point sources are classified as candidate HMXBs by Sturm et al. (2013).

In this paper, we selected seven of the most likely HMXB candidates from the X-ray classification by Sturm et al. (2013) for follow-up optical spectral and temporal analysis. From this analysis, we confirm these candidates as Be X-ray binaries in the SMC. In Section 2, we present the photometric and spectroscopic data used in the analysis, while in Section 3, we discuss the selection criteria and analysis techniques. Our results are presented in Section 4, while conclusions are discussed in Section 5.

2 DATA

2.1 Spectroscopy from ESO

Spectra were taken between 2011 December 9 and 10 with the ESO Faint Object Spectrograph (EFOSC2) mounted at the Nasmyth B focus of the 3.58-m New Technology Telescope. A slit width of 1.5 arcsec was employed, together with a grating ruled at 6001 mm^{-1}, which yielded 1 Å pixel^{-1} dispersion over a wavelength range of λλ3095–5085 Å. Spectra were recorded with exposure times between 300 and 800 s depending on source brightness, at a spectral resolution of ∼10 Å .

★ E-mail: vanessa@saao.ac.za

Table 1. Summary of observations. The first column 'Campaign' is used to identify the setup for each individual source listed in Table 3.

Campaign	Telescope	Dates	Wavelength range (Å)	Resolution (Å)
ESO07	ESO 3.6 m, La Silla, Chile	2007 September 19–20	3082–5087	4
ESO11	ESO NTT, La Silla, Chile	2011 December 9–10	3095–5085	10
AAT	AAT, Siding Spring, Australia	2012 July 7–8	4025–4775	1.2

We also utilized archival spectra of two objects observed on 2007 September 20 with EFOSC2 mounted on the European Southern Observatory (ESO) 3.6-m telescope at La Silla. In this case, a slit width of 1.0 arcsec was employed with all other instrument parameters the same as above. Typical exposure times ranged between 1000 and 1500 s.

All data were reduced using the standard packages available in the Image Reduction and Analysis Facility (IRAF[1]). Wavelength calibration was achieved with helium and argon arc lamps.

2.2 Spectroscopy from AAO

The Anglo-Australian Telescope (AAT) spectra were obtained with the fibre-fed dual-beam AAOmega spectrograph on the 3.9-m AAT at the Australian Astronomical Observatory (AAO) on 2012 July 7–8. The Two-degree Field ('2dF') multiobject system was utilized. Light from an optical fibre of diameter 2.1 arcsec on the sky is fed into two arms via a dichroic beam-splitter with a crossover at 5700 Å. Each arm of the AAOmega system is equipped with a 2k × 4k E2V CCD detector and an AAO2 CCD controller. The blue arm CCD is thinned for an improved blue response. Because of the atmospheric diffraction, our targets did not produce useful spectra on the red arm, which was observed around the infrared Ca II triplet for a different programme. We used grating 580 V, giving $R = 1300$ over ∼2100 Å. The central wavelength was set at 4500 Å.

We used the standard reduction pipeline 2DFDR as provided by the AAT at the time, with wavelength calibration by observing arc lamps before each target exposure. The arc lamps provide lines of He + CuAr + FeAr + ThAr + CuNe, and only those lines actually detected in the calibration exposures were input into the data reduction pipeline. The wavelength calibration was excellent, with the rms consistently <0.1 pixel.

Sky subtraction was carried out by means of a mean sky spectrum, obtained by averaging the spectra of 30 fibres positioned at known blank locations. The sky lines in each spectrum are evaluated and used to scale the mean sky spectrum prior to subtraction.

The journal of the spectroscopic observations is presented in Table 1.

2.3 Photometry from OGLE

The OGLE project[2] (see e.g. Udalski, Kubiak & Szymanski 1997; Udalski, Szymański & Szymański 2015) provides long-term *I*-band photometry with roughly daily sampling. These data were used to study the time variability of the optical counterparts to the candidate HMXBs. All of the HMXB candidates have been observed with OGLE III and IV. The OGLE identifications and light curve characteristics are presented in Table 2 and the OGLE IV light curves in Fig. 1.

Table 2. OGLE III and IV identifications and variability parameters. δI is the mean error on the data points, whereas ΔI represents the total range of the data set.

XMM ID	*I* band average mag	δI (mmag)	ΔI (mmag)	OGLE III ID	OGLE IV ID
12	15.53	5	105	SMC121.8 55	SMC733.202992
337	14.42	3	682	SMC105.6.39454	SMC726.32 26912
1400	14.90	4	955	SMC100.4.62974	SMC719.03.43645
1859	14.82	3	867	SMC103.7.6594	SMC720.11 13342
2208	16.92	7	273	SMC108.5 8790	SMC719.26 20124
2300	14.45	3	178	SMC105.5 37304	SMC719.18 7
3285	15.70	5	1246	SMC110.5 9503	SMC726.28 23178

3 ANALYSIS

3.1 Criteria for identification as a massive X-ray binary

Starting with the list of massive X-ray binary candidates in table 5 of Sturm et al. (2013), and excluding any objects previously confirmed as X-ray binary systems, we applied the following criteria:

(i) The X-ray source must belong to confidence class 2 or 3 – description below.
(ii) The optical counterpart must be a spectroscopically confirmed early-type star.

The confidence classes listed above were introduced by Haberl & Sturm (2016) in their classification of X-ray binaries in the SMC. Class 2 corresponds to an X-ray object showing significant X-ray variability (≥a factor of 30) or a hard power-law spectrum, but no X-ray pulsations. Class 3 corresponds to an X-ray source with an error circle small enough to identify it unambiguously with an early-type star showing emission lines.

Though we do not require a detected period in the optical light curve to classify an object as an HMXB, some systems do exhibit strong evidence for binary modulation. However, we also note that many HMXB systems do not exhibit this modulation (Bird et al. 2012). As a result of the above selection criteria, we present here six new HMXB systems.

3.2 Spectral classification

The motivation for and the method of spectral classification have been outlined in section 4 of McBride et al. (2008). We show in Fig. 2 the spectra we classified in this work. Spectral classifications can be found in Table 3.

[1] IRAF is distributed by the National Optical Astronomy Observatory, which is operated by the Association of Universities for Research in Astronomy (AURA) under cooperative agreement with the National Science Foundation.
[2] http://ogle.astrouw.edu.pl

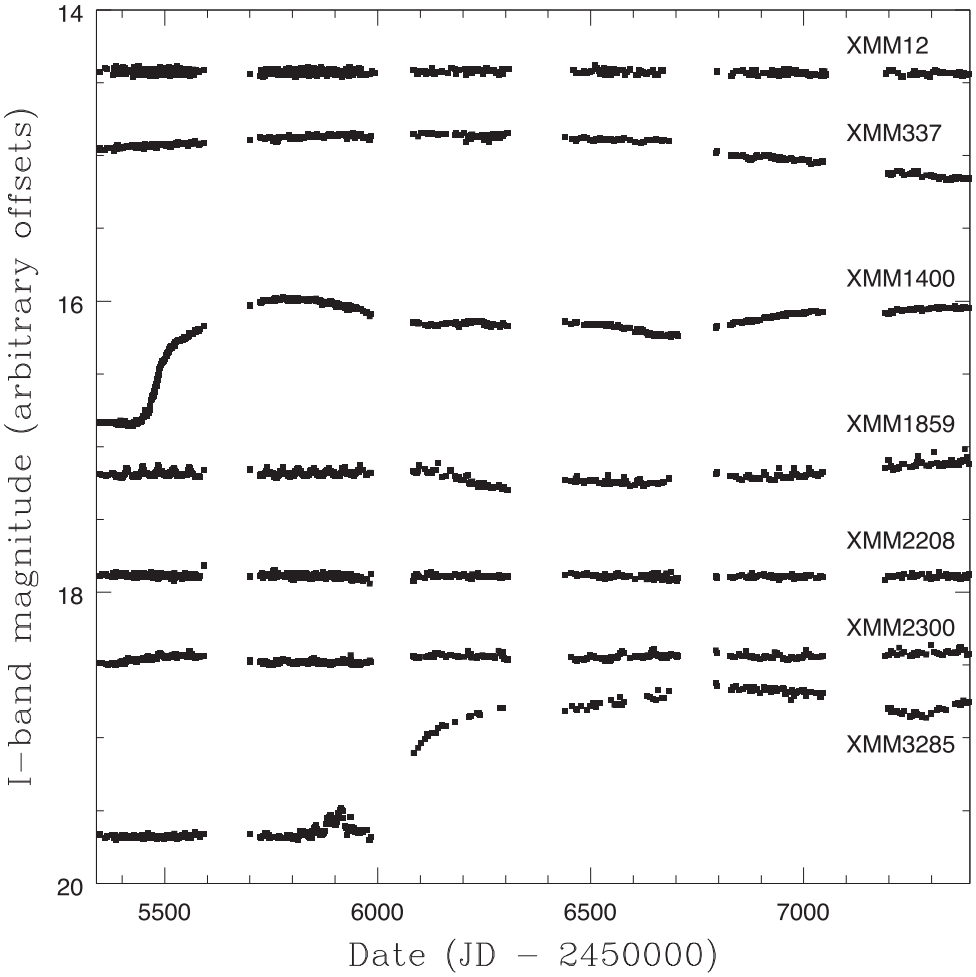

Figure 1. OGLE IV light curves of our six HMXB candidates and XMM 2300 to illustrate the extent of variability in the light curves.

3.3 Timing analysis

The OGLE data sets used in this analysis are listed in Table 2 and provide *I*-band photometry over many years.

The optical light curves were subject to detrending and period searching following the method explained in sections 2 and 3 of Bird et al. (2012). The results of this timing analysis are presented in Table 3.

4 DISCUSSION

4.1 Spectroscopy results

In Table 3, we present spectral classifications of the optical counterparts to seven X-ray sources. Six of the candidate X-ray binaries are now confirmed HMXBs, while XMM 2300 has already been identified in Sturm et al. (2013) as an X-ray source corresponding to a Be star (Evans et al. 2006). In all cases, the counterpart is classified as a B star, confirming the HMXB nature of the system and validating the X-ray and optical selection criteria used by Sturm et al. (2013). The spectra are illustrated in Fig. 2. Our spectral type of XMM 337 is confirmed by Evans et al. (2004), but the same authors find a slightly earlier spectral type (O9.5 V, their object #705) for XMM 1859, while Lamb et al. (2016) find a spectral type of O9 IIIe for XMM 1859. For XMM 1400, Lamb et al. (2013) find a spectral type of B0 Ve. Our classification of XMM 2300 confirms that of Evans et al. (2006).

Two spectra, XMM 2208 and XMM 3285, do not show emission in the Hβ line. XMM 2208 has shown strong Hα in emission in previous observations (Novara et al. 2011). Be stars are known to undergo disc-loss phases, where the Balmer lines appear entirely in absorption, so despite the lack of emission lines, the optical period, *V* magnitude and shallow Hβ absorption line (compared with the other Balmer lines in this source) all point strongly towards a Be X-ray binary nature of XMM 3285.

4.2 Timing results

Bird et al. (2012) show that there can be a confusion between short-period ($\leq$1 d) non-radial pulsations (NRPs) and longer period (>10 d) orbital modulation when the approximately daily sampling period beats with the NRP period and results in long period peaks in the periodogram. A case in point is XMM 3285, where a 37.15 d period reported by Rajoelimanana et al. (2011) was associated with aliasing of a possible shorter period modulation (Schmidtke et al. 2013).

An effective discriminant between aliased NRPs and orbital modulation is the shape of the folded light curve. The orbital modulation, probably caused by the neutron star disturbing the Be star circumstellar disc, typically shows a fast rise with an exponential decay, whereas NRPs have more sinusoidal profiles in the light curves. These characteristics can be reflected by two metrics: the phase asymmetry of the folded light curves and the phase full width at

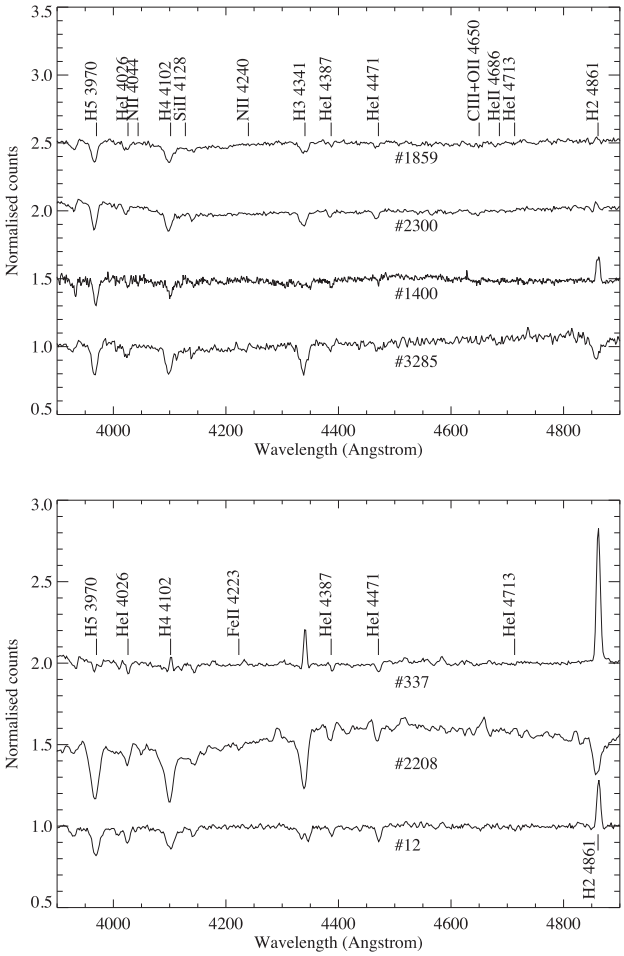

Figure 2. The top panel shows those spectra classified as B0–B1 in this work. The lower panel shows those classified as later than B1.

half-maximum (Bird et al. 2012) with the parameter space shown in Fig. 3.

From this plot, it can be seen that only sources XMM 1859 and XMM 2300 show strong evidence for the presence of a modulation that seems incompatible with the sinusoidal behaviour associated with NRP behaviour. Consequently, we present these results as clear evidence for binary modulation. Source XMM 3285 is marginal, whereas XMM 12 is a clear NRP candidate. XMM 12 exhibits two periods, at 0.55 d and at 5.18 d. Both periods are plotted, and lie on top of each other, in Fig. 3.

5 CONCLUDING REMARKS

In this work, we have presented an optical spectroscopic and timing analysis of candidate HMXBs in the SMC that generally exhibit low X-ray luminosities. The observations presented confirm the Be X-ray binary nature of these six candidates. We find evidence of two probable binary periods: 36.4 d in XMM 1859 and 72.2 d in XMM 2300. All candidates have early spectral types, as expected from the selection criteria applied in the original candidate HMXB list by Sturm et al. (2013).

Recently, a spin period of 15.6 s was discovered in XMM 1859 (Vasilopoulos et al. 2016), illustrating that the Be X-ray binaries as selected by this sample have properties consistent with those of the general population of Be X-ray binaries in the SMC. It is likely that they have been previously undetected as they have never been observed during an X-ray bright phase. *Swift* has just started regular monitoring of the SMC (Evans, Kenna & Coe 2016), and this improved sensitivity together with a wide area coverage may unearth more Be X-ray binary systems that have eluded detection up until now.

ACKNOWLEDGEMENTS

This paper is based on ESO data from 079.D−0371 and 088.D−0352. The AAT observations have been supported by the OPTICON project (observing proposals 2011A/014 and 2012/A015), which is funded by the European Commission under the Seventh Framework Programme (FP7). VAM acknowledges financial support from the National Research Foundation of South Africa (Grant 93405) and the World Universities Network. RD, AM and IN from the University of Alicante acknowledge support from the Spanish Government Ministerio de Economía y Competitividad under grant AYA2015-68012-C2-2-P (MINECO/FEDER). ESB acknowledges support from a Claude

Table 3. Results from optical spectroscopy and OGLE data timing analysis. Note that there are two periods seen in source XMM 12, and that the periodicity seen in source No. 3285 is only visible in one year's worth of data covering the period MJD 55650−56100.

XMM ID	RA (J2000)	Dec. (J2000)	*V* mag MCPS	Campaign	Spectral type (this work)	Period (d)	Detrending (d)	Previously referenced
12	01 19 38.94	−73 30 11.4	15.8	ESO07	B1.5–B2 III-Ve	0.552 2541(18) 5.183 31(24)	81 81	[SG05]28, [MA93]1867, [HS00]60
337	00 56 14.65	−72 37 55.8	14.6	ESO07	B3 IIIe or earlier	–	81	[SG05]22, [MA93]922, [E04]1135
1400	00 53 41.76	−72 53 10.1	14.7	AAT	B0.5–B1 IIIe	–	81	Lamb et al. (2013)
1859	00 48 55.55	−73 49 46.4	14.9	ESO11	B0 IV-Ve	36.432(9)	81	[E04]705, Lamb et al. (2016) Coe et al. (2016)
2208	00 56 05.48	−72 00 11.1	16.7	ESO11	B2–B3 Ve	–	81	Novara et al. (2011)
2300[a]	00 56 13.87	−72 29 59.7	14.5	ESO11 + AAT	B0.5 IVe	72.231(35)	101	Evans et al. (2006)
3285	01 04 29.42	−72 31 36.5	15.8	ESO11 + AAT	B1 V	29.75(18)	41	Rajoelimanana, Charles & Udalski (2011), Schmidtke, Cowley & Udalski (2013)

Notes. MCPS: Magellanic Clouds Photometric Survey: Zaritsky et al. (2002), SG05: Shtykovskiy & Gilfanov (2005), MA93: Meyssonnier & Azzopardi (1993), HS00: Haberl & Sasaki (2000) and E04: Evans et al. (2004).

[a]THIS SOURCE IS A PREVIOUSLY KNOWN HMXB (STURM ET AL. 2013) AND WE REPORT HERE OUR SPECTRAL CLASSIFICATION AND PERIODICITY.

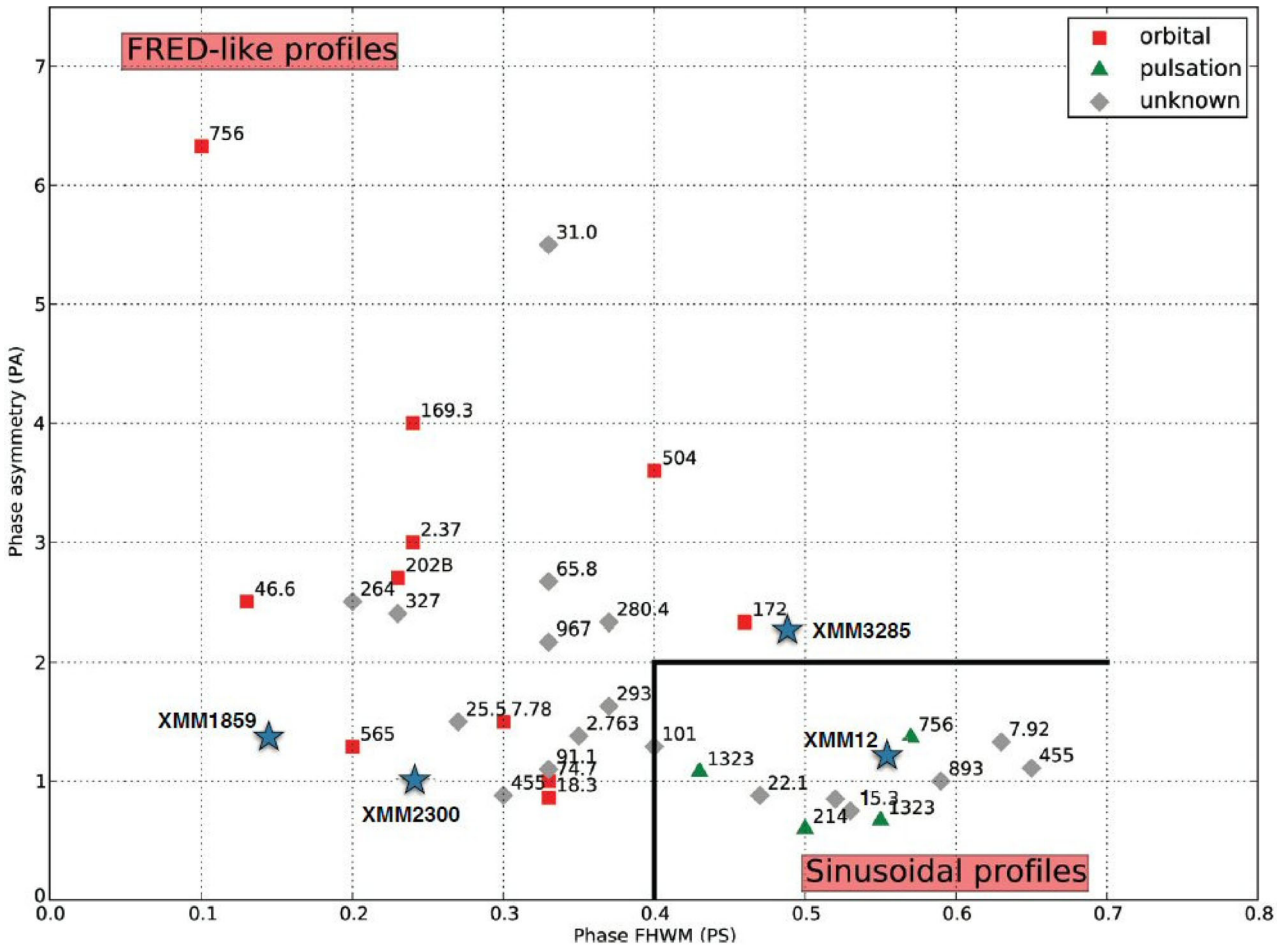

Figure 3. The parameter space for discriminating between aliased non-radial pulsations and orbital modulations in terms of the metrics phase asymmetry and phase FWHM (Bird et al. 2012). This figure shows the positions of the four sources exhibiting periodicities from this work against the background of all the previous sources studied in this way by Bird et al. (2012). Previous sources are all confirmed Be X-ray binaries and are labelled by their neutron star spin periods (in seconds).

Leon Foundation fellowship and from the Marie Curie Actions of the European Commission (FP7-COFUND). The OGLE project has received funding from the National Science Centre, Poland, grant MAESTRO 2014/14/A/ST9/00121 to AU.

REFERENCES

Antoniou V., Zezas A., 2016, MNRAS, 459, 528
Antoniou V., Hatzidimitriou D., Zezas A., Reig P., 2009, ApJ, 707, 1080
Bird A. J., Coe M. J., McBride V. A., Udalski A., 2012, MNRAS, 423, 3663
Coe M. J., McBride V., Haberl F., Bird A., Udalski A., 2016, The Astronomer's Telegram, 9198
Dray L. M., 2006, MNRAS, 370, 2079
Evans C. J., Howarth I. D., Irwin M. J., Burnley A. W., Harries T. J., 2004, MNRAS, 353, 601
Evans C. J., Lennon D. J., Smartt S. J., Trundle C., 2006, A&A, 456, 623
Evans P. A., Kenna J. A., Coe M. J., 2016, The Astronomer's Telegram, 9197
Haberl F., Sasaki M., 2000, A&A, 359, 573
Haberl F., Sturm R., 2016, A&A, 586, A81
Haberl F. et al., 2012, A&A, 545, A128
Hilditch R. W., Howarth I. D., Harries T. J., 2005, MNRAS, 357, 304
Lamb J. B., Oey M. S., Graus A. S., Adams F. C., Segura-Cox D. M., 2013, ApJ, 763, 101
Lamb J. B., Oey M. S., Segura-Cox D. M., Graus A. S., Kiminki D. C., Golden-Marx J. B., Parker J. W., 2016, ApJ, 817, 113
McBride V. A., Coe M. J., Negueruela I., Schurch M. P. E., McGowan K. E., 2008, MNRAS, 388, 1198
Meyssonnier N., Azzopardi M., 1993, A&AS, 102, 451
Negueruela I., 1998, A&A, 338, 505
Negueruela I., Coe M. J., 2002, A&A, 385, 517
Novara G. et al., 2011, A&A, 532, A153
Portegies Zwart S. F., 1995, A&A, 296, 691
Rajoelimanana A. F., Charles P. A., Udalski A., 2011, The Astronomer's Telegram, 3154
Schmidtke P. C., Cowley A. P., Udalski A., 2013, MNRAS, 431, 252
Shtykovskiy P., Gilfanov M., 2005, MNRAS, 362, 879
Sturm R. et al., 2013, A&A, 558, A3
Udalski A., Kubiak M., Szymanski M., 1997, Acta Astron., 47, 319
Udalski A., Szymański M. K., Szymański G., 2015, Acta Astron., 65, 1
Vasilopoulos G., Haberl F., Antoniou V., Zezas A., 2016, The Astronomer's Telegram, 9229
Zaritsky D., Harris J., Thompson I. B., Grebel E. K., Massey P., 2002, AJ, 123, 855

This paper has been typeset from a TEX/LATEX file prepared by the author.